

Journal of Organometallic Chemistry, 304 (1986) 227–238
 Elsevier Sequoia S.A., Lausanne – Printed in The Netherlands

SYNTHESIS AND CRYSTAL STRUCTURE OF A CARBOMETHOXY COMPLEX OF PENTACOORDINATE IRIDIUM(I), $\text{MeOC(O)Ir(CO)}_2(\text{PPh}_3)_2$

MELVYN ROWEN CHURCHILL *, JAMES C. FETTINGER, WAYNE M. REES and JIM D. ATWOOD

Department of Chemistry, University at Buffalo, State University of New York, Buffalo, New York 14214 (U.S.A.)

(Received October 16th, 1985)

Summary

The pentacoordinate complex $\text{MeOC(O)Ir(CO)}_2(\text{PPh}_3)_2$, prepared by carbonylation of *trans*-MeOIr(CO)(PPh₃)₂, crystallizes in the centrosymmetric triclinic space group $P\bar{1}$ with a 10.019(2), b 11.828(3), c 16.578(5) Å, α 103.83(2), β 92.71(2), γ 114.27(2)°, V 1715(1) Å³ and Z = 2. Diffraction data were collected and the structure was solved and refined to R 4.9% for 4504 reflections with $2\theta = 4.5\text{--}45.0^\circ$ (Mo- K_α), and R 3.6% for those 3768 data with $|F_0| > 6\sigma(|F_0|)$. The iridium(I) atom is in a trigonal-bipyramidal coordination environment. Axial bond lengths are Ir–CO₂Me 2.073(9) and Ir–P(2) 2.360(2) Å; equatorial bond lengths are Ir–P(1) 2.392(2), Ir–CO(1) 1.891(8) and Ir–CO(2) 1.895(10) Å. Isomerism in trigonal-bipyramidal molecules is discussed.

Introduction

We have previously described a convenient synthesis of *trans*-MeIr(CO)(PPh₃)₂ and its carbonylation to the five-coordinate acetyl complex MeC(O)Ir(CO)₂(PPh₃)₂ [1]. More recently we have extended this work to define a series of iridium alkoxide complexes, *trans*-ROIr(CO)(PPh₃)₂ and have reported their carbonylation to the five-coordinate carboalkoxy complexes ROC(O)Ir(CO)₂(PPh₃)₂ [2,3]. We have previously described the results of X-ray structural studies on the parent methyl and phenoxy species *trans*-MeIr(CO)(PPh₃)₂ [1] and *trans*-PhOIr(CO)(PPh₃)₂ [2]; we now report the detailed synthesis and the X-ray crystallographic analysis of the carbomethoxy complex, MeOC(O)Ir(CO)₂(PPh₃)₂.

* Address correspondence to this author.

Experimental

Preparation of MeOC(O)Ir(CO)₂(PPh₃)₂. A solution of 0.20 g *trans*-MeOIr-(CO)(PPh₃)₂ [3] in 20 ml dried toluene was prepared in an inert atmosphere glove box and transferred to a pressure bottle. The pressure bottle was sealed, removed from the glove box, flushed, charged with CO (50 psi) and allowed to stir at room temperature for 2 d. The solution was filtered and transferred to a vapor diffusion crystallization apparatus charged with dried pentane and stored under CO for 5 d yielding 0.13 g of pale yellow crystals (61% yield). Microanalysis: Found: C, 57.65; H, 3.82; P, 7.37. calcd.: C, 57.75; H, 3.97; P, 7.46%. IR (C₆H₆): 1994 s, 1939 vs, 1636 m cm⁻¹. (The IR spectrum in KBr is essentially identical to that observed in benzene, absorptions now being at 1982 s, 1935 vs and 1636 m cm⁻¹.)

¹H NMR (toluene-d₆): 3.00(s), 7.0(m) ppm.

Collection of the X-ray diffraction data

The crystal selected for the structural analysis was a very pale yellow, approximately equidimensional, parallelepiped of side ~ 0.2 mm. The crystal was sealed into a 0.2 mm diameter thin-walled glass capillary, was mounted on a eucentric goniometer and was accurately centered and aligned on a Syntex P2₁ automated four-circle diffractometer. All subsequent set-up operations (i.e., determination of unit cell parameters and the crystal's orientation matrix) and collection of the

TABLE 1

EXPERIMENTAL DATA FOR THE X-RAY DIFFRACTION STUDY OF MeOC(O)Ir(CO)₂(PPh₃)₂

(A) Crystallographic parameters at 24°C (297 K)

Crystal system: triclinic	Space group: P $\bar{1}$
<i>a</i> 10.019(2) Å	<i>V</i> 1715(1) Å ³
<i>b</i> 11.828(3) Å	<i>Z</i> 2
<i>c</i> 16.578(5) Å	formula C ₄₀ H ₃₃ IrO ₄ P ₂
α 103.83(2)°	mol. wt. 831.84
β 92.71(2)°	<i>D</i> (calcd.) 1.61 g cm ⁻³
γ 114.27(2)°	μ (Mo-K _α) 42.6 cm ⁻¹

(B) Measurement of intensity data

Diffractometer: Syntex P2₁

Radiation: Mo-K_α (λ 0.71073 Å)

Monochromator: highly oriented (pyrolytic) graphite in equatorial mode with 2θ (mono) = 12.160° for the 002 reflection; assumed to be 50% perfect/50% ideally mosaic for polarization correction

Reflections measured: + *h*, ± *k*, ± *l* for 2θ = 4.5°–45.0°; 4963 reflections collected and merged to 4504 unique data

Scan conditions: coupled θ (crystal)– 2θ (counter) at 4.0 deg/min (in 2θ) over the range [$2\theta(K_{\alpha_1}) - 0.9$]° → [$2\theta(K_{\alpha_2}) + 0.9$]°

Backgrounds: stationary crystal and counter at each extreme of the 2θ scan; each for one-fourth total scan time

Standard reflections: 3 approximately mutually orthogonal reflections were collected after every 97 data points; no significant fluctuations or decay were observed

Absorption correction: empirical, based upon interpolation (in 2θ and ϕ) between normalized ψ -scans of three close-to-axial reflections

intensity data (via a coupled θ (crystal)- 2θ (counter) scan routine) were performed as described previously [4]. Details appear in Table 1. The final unit cell parameters were based on a least-squares analysis of the setting angles (2θ , ω , χ) of the unresolved Mo- K_{α} components of 25 automatically centered reflections with $2\theta = 21\text{--}29^\circ$.

The crystal showed only C_i ($\bar{1}$) diffraction symmetry, with no systematic absences. It therefore belongs to the triclinic system, possible space groups being the noncentrosymmetric $P\bar{1}$ (C_1^1 ; No. 1) or the centrosymmetric $P\bar{1}$ (C_i^1 ; No. 2); the observation that $Z = 2$, the distribution of $|E|$ values and the successful solution of the structure in this higher space group all confirmed the latter centrosymmetric possibility.

All data were corrected empirically for absorption (against a set of normalized ψ -scans of 3 close-to-axial reflections) and for Lorentz and polarization effects and were converted to unscaled $|F_0|$ values. Data were placed on an approximately absolute scale by means of a Wilson plot.

Solution and refinement of the structure

All calculations were performed using the SUNY-Buffalo modified version of the Syntex XTL interactive crystallographic program package on a NOVA 1200 computer [5]. Scattering factors for neutral atoms (Ir, P, O, C, H) were used in their analytical form [6a]; the contributions of all non-hydrogen atoms were corrected for both the real ($\Delta f'$) and imaginary ($i\Delta f''$) components of anomalous dispersion [6b]. The function minimized during the least-squares refinement process was $\Sigma w(|F_0| - |F_c|)^2$, where $w^{-1} = [\sigma(|F_0|)]^2 + [0.015|F_0|]^2$.

The position of the iridium atom was determined from a Patterson map. All non-hydrogen atoms were located from difference-Fourier syntheses. Phenyl hydrogens were input at calculated positions (based on $d(\text{C-H})$ 0.95 Å [7] and externally-bisecting trigonal geometry), while hydrogen atoms of the methyl group were located from a difference-Fourier synthesis and were semi-idealized to C-H 0.95 Å. These positions were updated but were not refined. Full-matrix least-squares refinement

of positional and thermal parameters (anisotropic for the $\text{P}_2\text{Ir}(\text{CO})_2\text{C}(\text{O})\text{OC}$ moiety and isotropic for phenyl groups) for all non-hydrogen atoms led to convergence with the following discrepancy indices for all 4504 reflections. $R_F = 100\Sigma||F_0| - |F_c||/\Sigma|F_0| = 4.9\%$. $R_{wF} = 100[\Sigma w(|F_0| - |F_c|)^2/\Sigma w|F_0|^2]^{1/2} = 4.2\%$. $GOF = [\Sigma w(|F_0| - |F_c|)^2/(NO - NV)]^{1/2} = 1.43$, where NO is the number of observations and NV is the number of variables.

For those 4070 reflections with $|F_0| > 3\sigma(|F_0|)$, $R_F = 4.0\%$ and $R_{wF} = 4.1\%$; for those 3768 data with $|F_0| > 6\sigma(|F_0|)$, $R_F = 3.6\%$ and $R_{wF} = 4.0\%$.

A final difference-Fourier synthesis showed no significant features; the structure is therefore both correct and complete. Final positional and thermal parameters are collected in Tables 2 and 3.

Description of the structure

The crystal consists of an ordered arrangement of discrete monomeric molecular units of $\text{MeOC(O)Ir}(\text{CO})_2(\text{PPh}_3)_2$; there are no unusually short intermolecular contacts. The overall molecular geometry and labelling of non-hydrogen atoms is depicted in Fig. 1. A stereoscopic view of the molecule appears as Fig. 2. Interatomic distances and angles are collected in Tables 4 and 5.

(Continued on p. 233)

TABLE 2

FINAL ATOMIC COORDINATES FOR MeOC(O)Ir(CO)₂(PPh₃)₂

Atom	x	y	z	B (Å ²)
Ir	0.27289(3)	0.13239(3)	0.23435(2)	
P(1)	0.08025(21)	0.16050(17)	0.30389(12)	
P(2)	0.20448(22)	-0.08875(19)	0.21921(12)	
C(1)	0.22333(85)	0.09291(71)	0.11632(51)	
O(1)	0.19883(73)	0.06917(59)	0.04359(38)	
C(2)	0.4553(10)	0.18117(80)	0.30291(53)	
O(2)	0.57013(73)	0.21227(68)	0.33986(46)	
C(3)	0.34829(91)	0.32575(79)	0.23910(53)	
O(3)	0.42510(87)	0.41995(61)	0.29531(43)	
O(4)	0.30137(68)	0.34521(50)	0.16744(35)	
C(4)	0.3280(12)	0.47452(85)	0.16910(64)	
C(11)	0.13464(78)	0.26802(68)	0.41283(45)	2.53(14)
C(12)	0.02851(86)	0.28911(76)	0.45789(51)	3.40(16)
C(13)	0.0717(10)	0.37476(85)	0.53725(56)	4.25(18)
C(14)	0.2204(10)	0.44116(86)	0.57301(57)	4.43(19)
C(15)	0.3238(10)	0.41708(83)	0.53078(55)	4.09(18)
C(16)	0.28409(87)	0.33382(76)	0.44927(50)	3.37(16)
C(21)	-0.00411(77)	0.23792(67)	0.24789(44)	2.43(13)
C(22)	-0.00247(90)	0.35546(78)	0.28556(52)	3.61(16)
C(23)	-0.0641(10)	0.41254(90)	0.23894(59)	4.67(19)
C(24)	-0.1277(10)	0.34956(91)	0.15595(60)	4.79(20)
C(25)	-0.1291(10)	0.23105(85)	0.11743(56)	4.31(18)
C(26)	-0.06504(88)	0.17711(77)	0.16301(51)	3.50(16)
C(31)	-0.08117(77)	0.02441(67)	0.31892(44)	2.50(14)
C(32)	-0.06209(82)	-0.03073(72)	0.38162(47)	3.00(15)
C(33)	-0.17799(88)	-0.13299(76)	0.39708(50)	3.42(16)
C(34)	-0.31657(93)	-0.18189(82)	0.35126(54)	4.00(17)
C(35)	-0.3396(10)	-0.12989(88)	0.28876(58)	4.54(19)
C(36)	-0.22239(90)	-0.02758(79)	0.27268(52)	3.70(17)
C(41)	0.29435(79)	-0.15610(69)	0.13914(46)	2.66(14)
C(42)	0.43160(92)	-0.07628(80)	0.12530(53)	3.73(17)
C(43)	0.5035(11)	-0.1251(10)	0.06651(63)	5.19(21)
C(44)	0.4374(11)	-0.25331(93)	0.02325(60)	4.96(20)
C(45)	0.3021(10)	-0.33417(83)	0.03631(55)	4.09(18)
C(46)	0.22982(89)	-0.28499(78)	0.09446(52)	3.68(17)
C(51)	0.00914(77)	-0.19971(67)	0.17978(44)	2.43(13)
C(52)	-0.05369(88)	-0.20031(77)	0.10176(50)	3.45(16)
C(53)	-0.1994(10)	-0.28383(84)	0.06889(56)	4.15(18)
C(54)	-0.2860(10)	-0.36559(83)	0.11061(55)	4.12(18)
C(55)	-0.22736(93)	-0.36627(81)	0.18709(55)	3.95(17)
C(56)	-0.07943(82)	-0.28179(71)	0.22219(47)	3.89(14)
C(61)	0.25096(76)	-0.13462(67)	0.31126(45)	2.38(14)
C(62)	0.28242(86)	-0.05048(75)	0.39173(50)	3.29(16)
C(63)	0.31493(90)	-0.08726(79)	0.46193(52)	3.69(17)
C(64)	0.3184(10)	-0.20379(86)	0.45050(57)	4.29(18)
C(65)	0.29062(91)	-0.28667(80)	0.37244(53)	3.84(17)
C(66)	0.25548(87)	-0.25229(75)	0.30134(50)	3.32(16)
H(4A)	0.2788	0.4735	0.1183	6.0
H(4B)	0.4315	0.5264	0.1748	6.0
H(4C)	0.2909	0.5094	0.2155	6.0
H(12)	-0.0736	0.2442	0.4336	6.0
H(13)	-0.0007	0.3884	0.5677	6.0

TABLE 2 (continued)

Atom	<i>x</i>	<i>y</i>	<i>z</i>	<i>B</i> (\AA^2)
H(14)	0.2501	0.5031	0.6267	6.0
H(15)	0.4245	0.4577	0.5573	6.0
H(16)	0.3578	0.3221	0.4190	6.0
H(22)	0.0403	0.3982	0.3431	6.0
H(23)	-0.0619	0.4943	0.2647	6.0
H(24)	-0.1708	0.3873	0.1247	6.0
H(25)	-0.1736	0.1874	0.0602	6.0
H(26)	-0.0625	0.0976	0.1361	6.0
H(32)	0.0333	0.0031	0.4144	6.0
H(33)	-0.1616	-0.1695	0.4395	6.0
H(34)	-0.3968	-0.2515	0.3624	6.0
H(35)	-0.4357	-0.1640	0.2567	6.0
H(36)	-0.2391	0.0073	0.2293	6.0
H(42)	0.4774	0.0126	0.1560	6.0
H(43)	0.5975	-0.0697	0.0566	6.0
H(44)	0.4864	-0.2868	-0.0166	6.0
H(45)	0.2575	-0.4233	0.0059	6.0
H(46)	0.1351	-0.3408	0.1034	6.0
H(52)	0.0044	-0.1431	0.0719	6.0
H(53)	-0.2406	-0.2845	0.0158	6.0
H(54)	-0.3868	-0.4220	0.0869	6.0
H(55)	-0.2871	-0.4239	0.2160	6.0
H(56)	-0.0397	-0.2809	0.2756	6.0
H(62)	0.2819	0.0315	0.3991	6.0
H(63)	0.3344	-0.0310	0.5171	6.0
H(64)	0.3407	-0.2278	0.4982	6.0
H(65)	0.2948	-0.3670	0.3658	6.0
H(66)	0.2349	-0.3100	0.2466	6.0

TABLE 3

FINAL ANISOTROPIC THERMAL PARAMETERS FOR $\text{MeOC(O)Ir(CO)}_2(\text{PPh}_3)_2$ ^a

Atom	<i>B</i> ₁₁	<i>B</i> ₂₂	<i>B</i> ₃₃	<i>B</i> ₁₂	<i>B</i> ₁₃	<i>B</i> ₂₃
Ir	2.361(14)	2.203(14)	2.183(14)	0.902(10)	0.1897(94)	0.718(10)
P(1)	2.421(85)	2.009(81)	2.032(83)	0.738(69)	0.033(66)	0.548(67)
P(2)	2.822(92)	2.510(89)	2.376(89)	1.353(76)	0.214(72)	0.725(72)
C(1)	3.47(39)	2.55(35)	2.43(40)	0.75(30)	0.92(30)	1.10(29)
O(1)	7.30(40)	5.10(34)	2.68(31)	2.40(30)	0.73(27)	1.38(26)
C(2)	3.26(42)	3.66(42)	3.47(42)	0.93(34)	-1.23(34)	0.30(33)
O(2)	3.98(34)	6.48(40)	7.04(42)	1.39(30)	-1.40(31)	1.67(33)
C(3)	3.57(41)	2.96(40)	3.21(41)	0.94(34)	0.66(33)	1.49(35)
O(3)	9.91(51)	2.75(30)	4.64(36)	-0.56(31)	-2.25(35)	1.09(28)
O(4)	6.65(36)	2.61(26)	3.86(30)	1.78(25)	-0.12(26)	1.24(22)
C(4)	6.97(59)	3.19(44)	6.03(57)	2.22(42)	1.52(46)	2.06(41)

^a These anisotropic thermal parameters are in standard Syntex XTL format and enter the expression for the calculated structure factor in the form: $\exp[-0.25(h^2a^{*2}B_{11} + k^2b^{*2}B_{22} + l^2c^{*2}B_{33} + 2hka^{*}b^{*}B_{13} + 2hla^{*}c^{*}B_{23})]$.

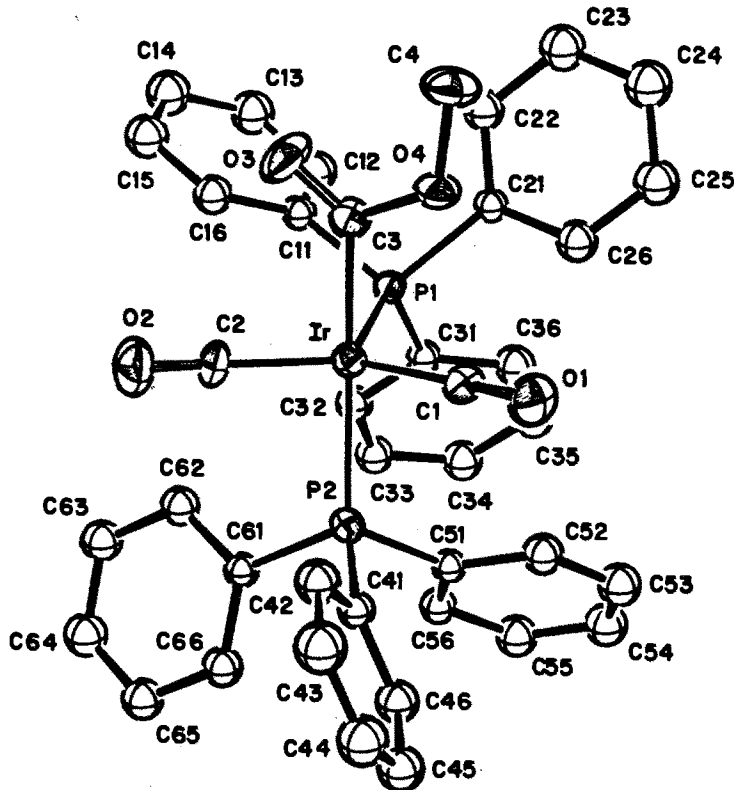


Fig. 1. Labelling of non-hydrogen atoms and molecular geometry of $\text{MeOC(O)}\text{Ir}(\text{CO})_2(\text{PPh}_3)_2$ [ORTEP-II diagram; 30% probability ellipsoids].

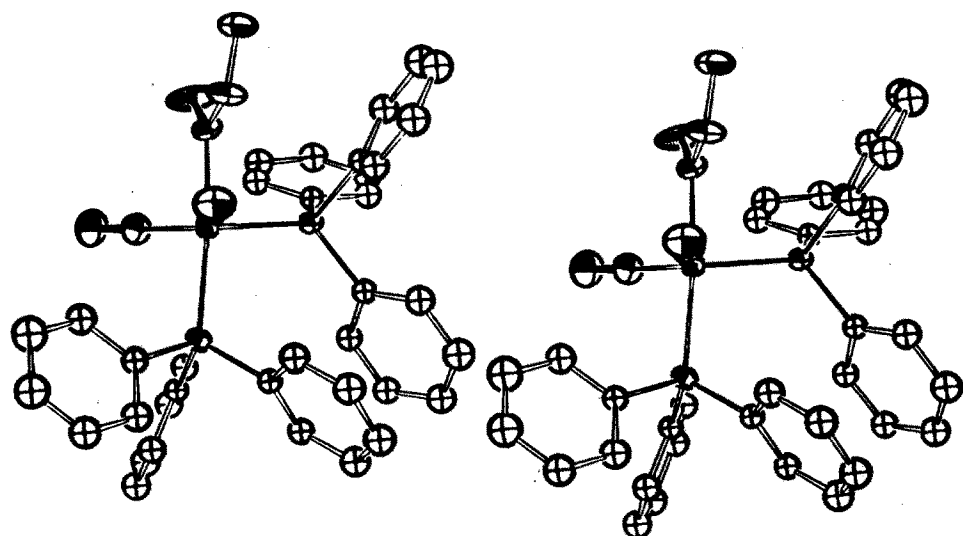


Fig. 2. Stereoscopic view of the $\text{MeOC(O)}\text{Ir}(\text{CO})_2(\text{PPh}_3)_2$ molecule.

TABLE 4
INTERATOMIC DISTANCES (Å) FOR MeOC(O)Ir(CO)₂(PPh₃)₂

(A) Metal-ligand distances			
Ir-P(1)	2.392(2)	Ir-C(1)	1.891(8)
Ir-P(2)	2.360(2)	Ir-C(2)	1.895(10)
		Ir-C(3)	2.073(9)
(B) Phosphorus-carbon distances			
P(1)-C(11)	1.848(7)	P(2)-C(41)	1.845(8)
P(1)-C(21)	1.839(8)	P(2)-C(51)	1.827(8)
P(1)-C(31)	1.833(8)	P(2)-C(61)	1.837(8)
P-C(average)	1.838 ± 0.007 ^a		
(C) Carbon-oxygen distances in Ir-CO systems			
C(1)-O(1)	1.160(10)	C(2)-O(2)	1.145(13)
(D) Carbon-oxygen distances in MeOC(O) systems			
C(3)-O(3)	1.197(11)	C(4)-O(4)	1.434(11)
C(3)-O(4)	1.361(10)		
(E) Carbon-carbon distances			
C(11)-C(12)	1.398(12)	C(41)-C(42)	1.379(13)
C(12)-C(13)	1.376(12)	C(42)-C(43)	1.393(14)
C(13)-C(14)	1.385(15)	C(43)-C(44)	1.364(15)
C(14)-C(15)	1.364(14)	C(44)-C(45)	1.364(15)
C(15)-C(16)	1.395(12)	C(45)-C(46)	1.392(13)
C(16)-C(11)	1.395(12)	C(46)-C(41)	1.377(12)
C(21)-C(22)	1.374(12)	C(51)-C(52)	1.409(11)
C(22)-C(23)	1.408(14)	C(52)-C(53)	1.374(13)
C(23)-C(24)	1.375(14)	C(53)-C(54)	1.361(13)
C(24)-C(25)	1.389(14)	C(54)-C(55)	1.375(13)
C(25)-C(26)	1.382(13)	C(55)-C(56)	1.399(13)
C(26)-C(21)	1.394(11)	C(56)-C(51)	1.379(11)
C(31)-C(32)	1.397(11)	C(61)-C(62)	1.392(11)
C(32)-C(33)	1.378(12)	C(62)-C(63)	1.404(12)
C(33)-C(34)	1.367(13)	C(63)-C(64)	1.361(13)
C(34)-C(35)	1.380(13)	C(64)-C(65)	1.360(13)
C(35)-C(36)	1.389(14)	C(65)-C(66)	1.409(12)
C(36)-C(31)	1.387(12)	C(66)-C(61)	1.382(12)
C-C(average)	1.384 ± 0.014 ^a		

^a Average distances are accompanied by esd's calculated by the "scatter formula":

$$\sigma(\text{aver}) = \left[\sum_{i=1}^{i=N} (d_i - \bar{d})^2 / (N-1) \right]^{1/2}$$

Here, \bar{d} is the mean of N "equivalent" measurements and d_i is the i^{th} such measurement.

The central iridium(I) atom is in a (slightly distorted) trigonal-bipyramidal coordination environment, with a triphenylphosphine ligand (centered on P(2)) and the carbomethoxy ligand (based on C(3)) occupying axial sites; the angle P(2)-Ir-C(3) is 174.0(3)°. Two carbonyl ligands (C(1)-O(1) and C(2)-O(2)) and a further triphenylphosphine ligand (centered on P(1)) take up the three equatorial sites; angles between the equatorial ligands are P(1)-Ir-C(1) 111.0(3), P(1)-Ir-C(2) 117.1(3) and C(1)-Ir-C(2) 130.8(4)°. These features are illustrated in Fig. 3.

Axial-equatorial angles are all fairly close to 90°, the largest being that between

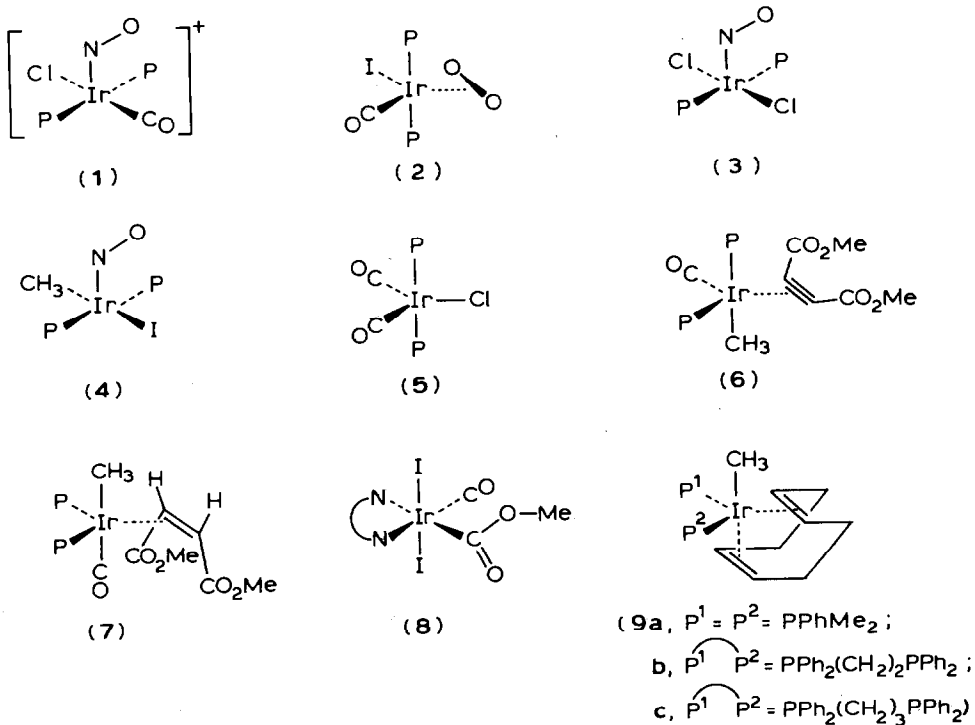
TABLE 5
INTERATOMIC ANGLES ($^{\circ}$) FOR $\text{MeOC(O)Ir(CO)}_2(\text{PPh}_3)_2$

<i>(A) Angles around the iridium atom</i>			
P(1)–Ir–P(2)	100.85(7)	P(2)–Ir–C(2)	91.5(3)
P(1)–Ir–C(1)	111.0(3)	P(2)–Ir–C(3)	174.0(3)
P(1)–Ir–C(2)	117.1(3)	C(1)–Ir–C(2)	130.8(4)
P(1)–Ir–C(3)	85.0(3)	C(1)–Ir–C(3)	87.6(4)
P(2)–Ir–C(1)	89.1(3)	C(2)–Ir–C(3)	86.9(4)
<i>(B) Ir–P–C and C–P–C angles</i>			
Ir–P(1)–C(11)	117.3(3)	C(11)–P(1)–C(21)	102.8(4)
Ir–P(1)–C(21)	109.8(3)	C(21)–P(1)–C(31)	103.1(4)
Ir–P(1)–C(31)	122.5(3)	C(31)–P(1)–C(11)	98.9(4)
Ir–P(2)–C(41)	112.0(3)	C(41)–P(2)–C(51)	101.0(4)
Ir–P(2)–C(51)	116.6(3)	C(51)–P(2)–C(61)	104.4(4)
Ir–P(2)–C(61)	118.1(3)	C(61)–P(2)–C(41)	102.6(4)
<i>(C) Ir–C–O angles for carbonyl ligands</i>			
Ir–C(1)–O(1)	177.2(8)	Ir–C(2)–O(2)	175.5(8)
<i>(D) Angles involving the MeOC(O) ligand</i>			
Ir–C(3)–O(3)	129.2(7)	O(3)–C(3)–O(4)	117.1(8)
Ir–C(3)–O(4)	113.8(6)	C(3)–O(4)–C(4)	117.9(7)
<i>(E) P–C–C angles</i>			
P(1)–C(11)–C(12)	120.8(6)	P(2)–C(41)–C(42)	119.3(6)
P(1)–C(11)–C(16)	119.7(6)	P(2)–C(41)–C(46)	121.7(6)
P(1)–C(21)–C(22)	122.4(6)	P(2)–C(51)–C(52)	117.7(6)
P(1)–C(21)–C(26)	118.1(6)	P(2)–C(51)–C(56)	123.7(6)
P(1)–C(31)–C(32)	118.2(6)	P(2)–C(61)–C(62)	120.0(6)
P(1)–C(31)–C(36)	124.6(6)	P(2)–C(61)–C(66)	120.5(6)
<i>(F) C–C–C angles</i>			
C(16)–C(11)–C(12)	119.4(8)	C(46)–C(41)–C(42)	119.0(8)
C(11)–C(12)–C(13)	120.1(8)	C(41)–C(42)–C(43)	120.5(9)
C(12)–C(13)–C(14)	120.5(9)	C(42)–C(43)–C(44)	119.3(10)
C(13)–C(14)–C(15)	119.7(9)	C(43)–C(44)–C(45)	121.2(10)
C(14)–C(15)–C(16)	121.1(9)	C(44)–C(45)–C(46)	119.4(9)
C(15)–C(16)–C(11)	119.1(8)	C(45)–C(46)–C(41)	120.5(8)
C(26)–C(21)–C(22)	119.4(8)	C(56)–C(51)–C(52)	118.6(7)
C(21)–C(22)–C(23)	120.1(8)	C(51)–C(52)–C(53)	119.7(8)
C(22)–C(23)–C(24)	119.8(9)	C(52)–C(53)–C(54)	121.5(9)
C(23)–C(24)–C(25)	120.4(10)	C(53)–C(54)–C(55)	119.9(9)
C(24)–C(25)–C(26)	119.5(9)	C(54)–C(55)–C(56)	119.9(8)
C(25)–C(26)–C(21)	120.8(8)	C(55)–C(56)–C(51)	120.5(8)
C(36)–C(31)–C(32)	117.3(7)	C(66)–C(61)–C(62)	119.5(7)
C(31)–C(32)–C(33)	121.7(8)	C(61)–C(62)–C(63)	119.7(8)
C(32)–C(33)–C(34)	120.0(8)	C(62)–C(63)–C(64)	119.7(8)
C(33)–C(34)–C(35)	119.9(9)	C(63)–C(64)–C(65)	121.7(9)
C(34)–C(35)–C(36)	120.1(9)	C(64)–C(65)–C(66)	119.4(9)
C(35)–C(36)–C(31)	121.1(8)	C(65)–C(66)–C(61)	120.0(8)
C–C–C(average)	120.0 ± 0.9 ^a		

^a See footnote to Table 4.

the two bulky triphenylphosphine ligands (P(1)–Ir–P(2) 100.85(7) $^{\circ}$); the P(2)–Ir–(equatorial ligand) angles range 89.1(3)–100.85(7) $^{\circ}$ while the C(3)–Ir–(equatorial ligand) angles are all acute (85.0(3)–87.6(4) $^{\circ}$).

The equatorial iridium–phosphorus bond length is slightly longer than the axial one (i.e., Ir–P(1) 2.392(2) as compared to Ir–P(2) 2.360(2) Å). These bond lengths are in the upper range of observed Ir–P distances (~ 2.25–2.45 Å) tabulated by Churchill and Bezman [8]. Ir– PPh_3 distances found in related pentacoordinate molecules containing the bis(triphenylphosphine) iridium moiety include the following: 2.407(3) and 2.408(3) Å in the square pyramidal $[\text{IrCl}(\text{CO})(\text{NO})(\text{PPh}_3)_2]^+$ cation (**1**) [9], 2.386(8) and 2.391(8) Å in the trigonal-bipyramidal $\text{IrI}(\text{O}_2)-(\text{CO})(\text{PPh}_3)_2$ (**2**) [10], 2.367(2) Å (twice) in the square-pyramidal $\text{IrCl}_2(\text{NO})(\text{PPh}_3)_2$ (**3**) [11], 2.348(3) Å (twice) in the square-pyramidal $\text{IrI}(\text{CH}_3)(\text{NO})(\text{PPh}_3)_2$ (**4**) [12], 2.322(7) and 2.341(7) Å in the trigonal-bipyramidal $\text{IrCl}(\text{CO})_2(\text{PPh}_3)_2$ (**5**) [13] 2.402(3) and 2.425(4) Å in the trigonal-bipyramidal $\text{Ir}(\text{CH}_3)(\text{CO})(\text{PPh}_3)_2(\text{MeO}_2\text{CC}\equiv\text{CO}_2\text{Me})$ (**6**) [14] and 2.344(2) and 2.376(2) Å in the trigonal-bipyramidal $\text{Ir}(\text{CH}_3)(\text{CO})(\text{PPh}_3)_2(\text{MeO}_2\text{CCH}=\text{CHCO}_2\text{Me})$ (**7**) [15]. In all of these species save **6**, **7** and the present complex, the PPh_3 ligands take up mutually *trans* sites.



The Ir–CO distances of 1.891(8) and 1.895(10) Å are in the normally expected range [9,10,13–15] and are substantially shorter than the iridium–carbomethoxy distance of 2.073(9) Å. This latter distance is in good agreement with that found in the octahedral iridium(III) carbomethoxy complex $\text{Ir}(\text{CO}_2\text{Me})\text{I}_2(\text{CO})(\text{bipy})$ (**8**), where Ir– CO_2Me 2.05(2) Å [16]. These Ir– CO_2Me bond lengths both appear to be significantly shorter than the typical iridium–alkyl bonds. Known *axial* Ir–CH₃ distances in trigonal-bipyramidal iridium(I) species include 2.193(14) in **6** [14], 2.159(8) in **7** [15], 2.202(22) in $(\text{cyclo-C}_8\text{H}_{12})(\text{PPhMe}_2)_2\text{IrMe}$ (**9a**) [17], 2.133(16) in $(\text{cyclo-C}_8\text{H}_{12})(\text{PPh}_2(\text{CH}_2)_2\text{PPh}_2)\text{IrMe}$ (**9b**) [18] and 2.153(18) Å in $(\text{cyclo-C}_8\text{H}_{12})(\text{PPh}_2(\text{CH}_2)_3\text{PPh}_2)\text{IrMe}$ (**9c**) [19].

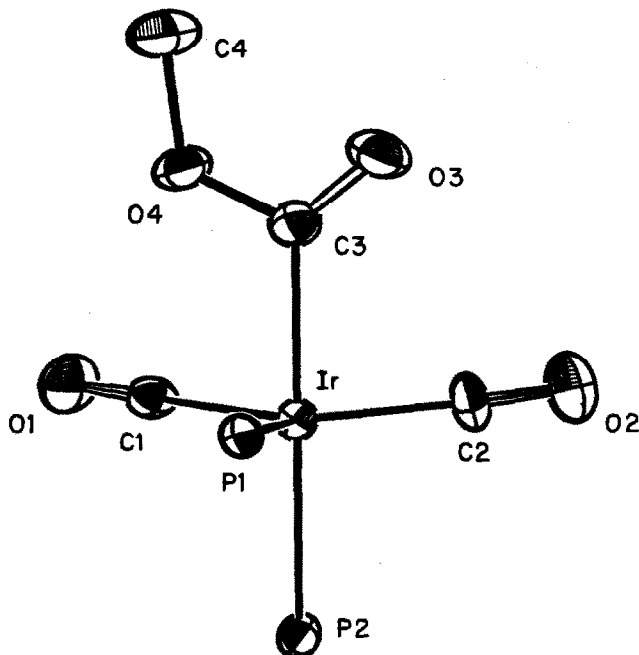


Fig. 3. The coordination environment of iridium(I) in $\text{MeOC(O)Ir(CO)}_2(\text{PPh}_3)_2$.

$\text{C}_8\text{H}_{12})(\text{PPh}_2(\text{CH}_2)_3\text{PPh}_2)\text{IrMe}$ (**9c**) [19].

Distances and angles in the carbomethoxy ligand are all in the expected ranges; the carbonyl function has a characteristic C=O bond length (C(3)-O(3) 1.197(11) Å), the C(3)-O(4) distance of 1.361(10) Å is typical of a $\text{C}(\text{sp}^2)$ -O single bond and the C(4)-O(4) distance of 1.434(11) Å is typical of a $\text{C}(\text{sp}^3)$ -O single bond. Angles about C(3) show slight variations from ideal trigonal geometry. The Ir-C(3)-O(3) angle of 129.2(7)° is the greatest of these, with Ir-C(3)-O(4) 113.8(6) and O(3)-C(3)-O(4) 117.1(8)°; the angle at O(4) is C(3)-O(4)-C(4) 117.9(7)°.

As can clearly be seen in the Figures, the C(3)-O(4) bond of the carbomethoxy ligand lies essentially over the carbonyl ligand C(1)-O(1), with a rather close C(carbonyl) ··· O(methoxy) contact of C(1) ··· O(4) 2.654(10) Å. (The C(1) ··· C(3) distance is 2.746(12) Å.) The former is consistent with an incipient weak interaction of the methoxy group with the carbonyl ligand as might occur at the beginning of a nucleophilic attack on the carbonyl ligand. However, the near-linearity of the Ir-C(1)-O(1) system (< 177.2(8)°) and a survey of the angles about O(4) (C(3)-O(4)-C(4) 117.9(7), C(1) ··· O(4)-C(3) 79.2(5) and C(1) ··· O(4)-C(4) 162.9(6)°) assures us that the interaction is very slight and that this portion of the molecule is little perturbed from a simple $\text{Ir}(\text{C}=\text{O})\text{OMe}(\text{CO})$ moiety. Interestingly, a similar situation is observed in the octahedral iridium(III) carbomethoxy complex $\text{Ir}(\text{CO}_2\text{Me})\text{I}_2(\text{CO})(\text{bipy})$ (**8**) [16].

The triphenylphosphine ligands are associated with Ir-P-C(*ipso*) angles greater than the ideal tetrahedral angle (i.e., ranging from 109.8(3) through 122.5(3)°), while the C-P-C angles vary from 98.9(4) through 104.4(4)°. The carbon atom skeletons of the phenyl rings show indications of the expected slight distortions from D_{6h} toward C_{2v} symmetry [20,21]. All remaining distances and angles are normal.

Discussion

Isomerism and ground state geometry in trigonal-bipyramidal complexes

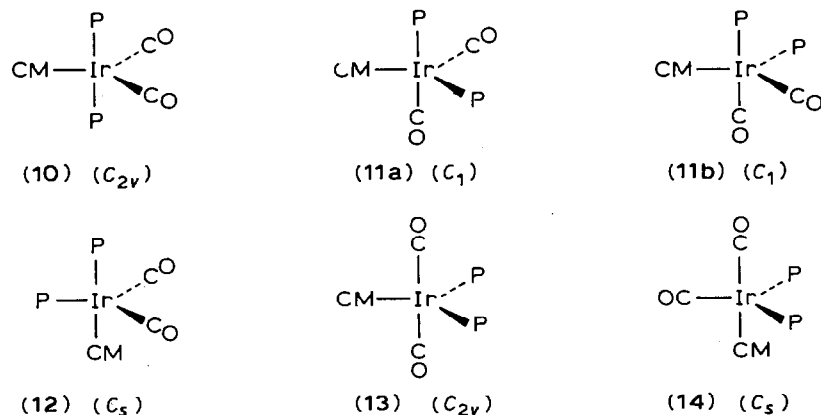
The number of possible diastereomers of a trigonal-bipyramidal complex may be determined simply from the number of different permutations of pairs of ligands that can be assigned to the axial positions. The most general case, Mabcde, thus yields ten diastereomers (each of which generates two enantiomers) with axial ligand pairs a–b, a–c, a–d, a–e, b–c, b–d, b–e, c–d, c–e and d–e.

There are five possible diastereomers (one of which is chiral and gives rise to an enantiomeric pair) for the present complex, $\text{MeOC(O)Ir(CO)}_2(\text{PPh}_3)_2$ (see Scheme 1). These are the P–P isomer (**10**), the P–CO enantiomeric pair (**11a** and **11b**), the P–CM (CM = carbomethoxy, $-\text{C}(\text{O})\text{OMe}$) isomer (**12**), the CO–CO isomer (**13**) and the CO–CM isomer (**14**); **12** corresponds to the stereochemistry actually determined from the present structural study.

Interconversion of isomers of pentacoordinate complexes is possible via the Berry pseudorotation mechanism and has been discussed by Shapley and Osborn [22]. (The “turnstile mechanism” [23] is permutationally equivalent and offers an alternative explanation, differing only in the route taken in the transit of ligands from one site to another.)

Providing that the barrier to interconversion of isomers is low, the observed product will be the “thermodynamic isomer”. (This is usually the case for Ir^{I} complexes.) The work of Shapley and Osborn [22] indicated that (in the absence of large ligand–ligand interactions) good σ -donors tended to occupy axial sites and that good π -acceptors tended to occupy equatorial sites. The theoretical treatment of Rossi and Hoffmann is consistent with these qualitative observations [24].

The known trigonal-bipyramidal five-coordinate derivatives of the *trans*- $\text{MeIr(CO)(PPh}_3)_2$ and *trans*- $\text{MeOIr(CO)(PPh}_3)_2$, viz., $\text{Ir(CH}_3)(\text{CO})(\text{PPh}_3)_2$ –($\text{MeO}_2\text{CC}\equiv\text{CCO}_2\text{Me}$) (**6**) [14], $\text{Ir(CH}_3)(\text{CO})(\text{PPh}_3)_2$ –($\text{MeO}_2\text{CCH=CHCO}_2\text{Me}$) (**7**) [15] and the present $\text{MeOC(O)Ir(CO)}_2(\text{PPh}_3)_2$ (**12**) each have the methyl or carbomethoxy ligands (good σ -donors) in axial sites. Complex **7** has both triphenyl-



Scheme 1. Possible isomers for trigonal-bipyramidal $\text{MeOC(O)Ir(CO)}_2(\text{PPh}_3)_2$ ($\text{P} = \text{PPh}_3$ and $\text{CM} = -\text{C}(\text{O})\text{OMe}$).

ylphosphine ligands in equatorial sites (presumably for steric reasons) and the carbonyl ligand in an axial site, while both **6** and **12** have a triphenylphosphine ligand in an axial site and the carbonyl ligands (one in **6**, two in **12**) in the more favorable equatorial sites. This competition between steric and electronic factors means that crystallographic studies will often be necessary to determine unequivocally the ground-state geometry of complex pentacoordinate iridium(I) species.

Additional Material

A table of observed and calculated structure factor amplitudes is available upon request from M.R.C.

Acknowledgments

We acknowledge the National Science Foundation and the Donors of the Petroleum Research Fund for partial support of this research. J.D.A. acknowledges the Alfred P. Sloan Foundation for a fellowship. W.R. acknowledges the Graduate School of SUNY for a fellowship. A loan of $\text{IrCl}_3 \cdot x\text{H}_2\text{O}$ was generously provided by Johnson Matthey Corporation.

References

- 1 W.M. Rees, M.R. Churchill, Y.J. Li and J.D. Atwood, *Organometallics*, **4** (1985) 1162.
- 2 W.M. Rees, M.R. Churchill, J.C. Fettinger and J.D. Atwood, *Organometallics*, **4** (1985) 2179.
- 3 W.M. Rees and J.D. Atwood, *Organometallics*, **4** (1985) 402.
- 4 M.R. Churchill, R.A. Lashewycz and F.J. Rotella, *Inorg. Chem.*, **16** (1977) 265.
- 5 Syntex XTL Operations Manual, 2nd Edit., Syntex Analytical Instruments, Cupertino, California, U.S.A. (1976).
- 6 International Tables for X-Ray Crystallography, Vol. 4, Kynoch Press, Birmingham, England, 1974; (a) pp. 99–101, (b) pp. 149–150.
- 7 M.R. Churchill, *Inorg. Chem.*, **12** (1973) 1213.
- 8 M.R. Churchill and S.A. Bezman, *Inorg. Chem.*, **13** (1974) 1418; see, particularly, Table VI on p. 1425.
- 9 D.J. Hodgson and J.A. Ibers, *Inorg. Chem.*, **7** (1968) 2345.
- 10 J.A. MGinnety, R.J. Doedens and J.A. Ibers, *Inorg. Chem.*, **6** (1967) 2243.
- 11 D.M.P. Mingos and J.A. Ibers, *Inorg. Chem.*, **10** (1971) 1035.
- 12 D.M.P. Mingos, W.T. Robinson and J.A. Ibers, *Inorg. Chem.*, **10** (1971) 1043.
- 13 N.C. Payne and J.A. Ibers, *Inorg. Chem.*, **8** (1969) 2714.
- 14 M.R. Churchill, W.M. Rees, J.C. Fettinger and J.D. Atwood, *Organometallics*, in press.
- 15 M.R. Churchill, J.C. Fettinger, W.M. Rees and J.D. Atwood, *J. Organomet. Chem.*, in press.
- 16 V.G. Albano, P.L. Bellon and M. Sansoni, *Inorg. Chem.*, **8** (1969) 298.
- 17 M.R. Churchill and S.A. Bezman, *Inorg. Chem.*, **11** (1972) 2243.
- 18 M.R. Churchill and S.A. Bezman, *Inorg. Chem.*, **12** (1973) 260.
- 19 M.R. Churchill and S.A. Bezman, *Inorg. Chem.*, **12** (1973) 531.
- 20 M.R. Churchill and B.G. DeBoer, *Inorg. Chem.*, **14** (1975) 2630.
- 21 A. Domenicano, A. Vaciago and C.A. Coulson, *Acta Cryst.*, **B31** (1975) 1630.
- 22 J.R. Shapley and J.A. Osborn, *Acc. Chem. Res.*, **6** (1973) 305.
- 23 I. Ugi, D. Marquarding, H. Klusacek, P. Gillespie and F. Ramirez, *Acc. Chem. Res.*, **4** (1971) 288.
- 24 A.R. Rossi and R. Hoffmann, *Inorg. Chem.*, **14** (1975) 365.